Journal of the Serbian Society for Computational Mechanics / Vol. 19 / No. 1, 2025 / pp 372-388 / review paper
(10.24874/jsscm.2025.19.01.23)

FINITE ELEMENT MODELING OF FLUID-STRUCTURE INTERACTION - APPLIED TO COCHLEAR MECHANICS

Velibor Isailovic [1,*] [0000-0002-1417-9633], Nenad Filipovic[1,2] [0000-0001-9964-5615] , Milica Nikolic[3] [0000-0002-8537-7944] and Milos Kojic[2,4] [0000-0003-2199-5847]

[1]Faculty of Engineering, University of Kragujevac, Sestre Janjic 6, 34000 Kragujevac, Serbia
[2]Bioengineering Research and Development Center BioIRC Kragujevac, Prvoslava Stojanovica 6, 3400 Kragujevac, Serbia.
[3]Institute of Information Technologies, University of Kragujevac, Department of Technical-Technological Sciences, Jovana Cvijica bb, 34000 Kragujevac, Serbia.
[4]Serbian Academy of Sciences and Arts, Knez Mihailova 35, 11000 Belgrade, Serbia
[*]Corresponding author

Abstract

This paper describes software developed based on numerical implementation of algorithms for coupled acoustic – structure interaction. This class of problems implies coupling of the fluid domain, with sound wave propagation, and the domain of solid, which vibrates under the pressure caused by sound waves from the fluid domain. The physical behavior of the solid domain is described by using Newtonian dynamic equations. On the other hand, sound wave propagation through the fluid domain is described by using the acoustic wave equation. The coupling of differential equations for these two different domains is accomplished by equalizing the most dominant forces from the both domains: inertial forces from the solid domain and pressure gradients from the fluid domain. As a result of scientific research, we present numerical software developed based on mentioned equations. The details of the equations and their coupling are given in the Methods section. The spatial discretization of equations is done by using the finite element method. The software is tested on benchmark examples found in literature (Beranek et al. 1992; Kojic et al. 2010). Additionally, the application of software in modeling of the problems in the field of biomedical engineering applied to cochlear mechanics is shown.

Keywords: Fluid-Structure Interaction, Cochlear mechanics, Finite element method

1. Introduction

Solid-fluid interaction problems are very widespread in different fields of science and technology. For example: aerodynamics of aircrafts or vehicles, fluid motion in tanks, fluid flow in tubes, blood flow in blood vessels, airflow in respiratory organs, sound wave propagation in hearing system, etc. Problems like this imply the presence of two different domains: fluid and solid. The fluid domain is usually described by the Navier – Stokes equations and the equation of continuity (Kojic et al. 2010; Kojic et al. 2008; Kojic et al. 2017;

Isailovic et al. 2014; Kojic et al. 2015). Unknown field variables in that case are the velocity and the pressure, or just velocity if a penalty formulation is used (Kojic et al. 2008). Besides, there is a class of problems where fluid flow is almost negligible, but the propagation of the acoustic waves (i.e. acoustic pressure) through the fluid medium is significant. These waves that travel through the fluid media can be described with the acoustic wave equation with the acoustic pressure as an unknown variable. In both cases, the first, where fluid flow and pressure distribution are significant, and the second, where only the sound wave propagation is significant, it is essential to take into account the influence of the fluid on the surrounding solid domain. The mechanical behavior of the solid domain is described by Newton's equations of motion with displacement as an unknown variable.

Different numerical methods or combinations of numerical methods can be applied to evaluate the mechanical behavior for arbitrary spatial domains. But, most commonly used is finite element method. For fluid domain there are several different techniques, such as the finite element method, finite volume method, finite difference method, spectral methods, etc. The focus of this paper is finite element method and its application on coupled problem: solid and fluid (acoustic) interaction. The finite element method will be used for both, solid and fluid, domains. As a starting point, software package PAK (Program for Analysis of Constructions, Kragujevac, Serbia, Kojic et al. 2017) is used. Basic functionalities necessary for numerical discretization are taken from this source. Moreover, for the solving of system of linear equations (obtained by the discretization) the MUMPS parallel solver is used (Amestroy et al. 1999).

Since the objective of this research was to develop numerical software, suitable examples have been used for its validation. Examples are found in literature and have analytical solution in closed form. Matching of the results obtained numerically (by developed software) with results obtained analytically is a proof of the accuracy of the software solution presented here.

2. Methods

The methods section will provide the basic equations implemented in the software. Also, the method of coupling of equations used for describing two different domains (fluid and solid) will be described.

For physical describing of the fluid flow, the Navier – Stokes equations are commonly used. However, in the propagation of sound waves through the fluid, fluid motion is not dominant since the Mach number is very small (M << 1). Bearing that in mind, the acoustic wave equation can be used for describing the sound wave propagation (ANSYS Theory Reference Release 5.6; Moand et al. 1995; Rienstra et al. 2009):

$$\frac{\partial^2 p}{\partial x_i^2} - \frac{1}{c^2}\frac{\partial^2 p}{\partial t^2} = 0 \tag{1}$$

where is: p – fluid pressure, c – speed of sound, x_i - spatial coordinates in Cartesian coordinate system ($i = 1,2,3$) and t – time. Using Galerkin method (Kojic et al. 2010), the equation (1) can be written in the matrix form:

$$\mathbf{Q}\ddot{\mathbf{p}} + \mathbf{H}\mathbf{p} = \mathbf{0} \tag{2}$$

where is:

$\mathbf{Q} = \frac{1}{c^2}\int_V \mathbf{N}^T \mathbf{N} dV$ – acoustic “inertia”,

$\mathbf{H} = \int_V \mathbf{N}'^T \mathbf{N}' dV$ – acoustic “stiffness”.

In the last two equations, the matrices $\boldsymbol{N}$ and $\boldsymbol{N}'$ contain linear shape functions and their derivatives (Bathe 1996, Kojic et al. 2008).

Starting from the principle of virtual work, that equalizes the virtual work of internal and external forces, and taking into account the influence of inertial and dissipative forces, the equation of solid motion (and deformation) can be defined in the following form:

$$\mathbf{M}\ddot{\mathbf{u}} + \mathbf{C}\dot{\mathbf{u}} + \mathbf{K}\mathbf{u} = \mathbf{F}^{\mathbf{ext}} \tag{3}$$

where is:

$\mathbf{M} = \int_V \rho \mathbf{N}^T \mathbf{N} dV$ – mass matrix,

$\mathbf{C} = \int_V c \mathbf{N}^T \mathbf{N} dV$ – damping matrix,

$\mathbf{K} = \int_V \mathbf{B}^T \mathbf{D} \mathbf{B} dV$ – stiffness matrix with elasticity matrix $\mathbf{D}$ and strain-displacement matrix $\mathbf{B}$,

$\mathbf{u}$ - displacement vector,

$\dot{\mathbf{u}}$ – velocity vector,

$\ddot{\mathbf{u}}$ – acceleration vector,

$\mathbf{F}^{\mathbf{ext}}$ – vector of external forces.

The details of equations given above can be found in literature (Zienkievicz 1983, Bathe 1996, Kojic et al. 2008).

In acoustics, it is often necessary to observe only the free response of the vibrating system, without damping. In that case, damping term in the dynamic equation can be omitted. Therefore, the equation can be reduced to a simpler form:

$$\mathbf{M}\ddot{\mathbf{u}} + \mathbf{K}\mathbf{u} = \mathbf{F}^{\mathbf{ext}} \tag{4}$$

The software for solving equations (3) or (4) is already done (Kojic et al. 2017) and that part of code is used here as a starting point. Since that code exists and has been thoroughly tested, this paper will not deal with validation of that.

The focus of this paper is developing of the finite element software for solving of equation (2) and coupling of equations (2) with (4) by additional equation that will be explained below.

Equations (2) and (4) can be coupled by introducing an additional equation (or, in other words, a boundary condition) which equalizes the most dominant forces from both domains: the inertial forces from solid domain and pressure gradient from fluid domain. Force equalization is performed in the direction of the normal of the boundary surface between the fluid and the solid domains (ANSYS Theory Reference Release 5.6; Morand et al. 1995; Zienkievicz 1983):

$$\mathbf{n} \cdot \nabla p = \rho \mathbf{n} \cdot \ddot{\mathbf{u}} \tag{5}$$

where is:

$\mathbf{n}$ – normal vector on fluid – structure interface (FSI),

∇p – gradient of fluid pressure,

ρ – density of fluid,

$\ddot{\mathbf{u}}$ – acceleration of solid.

Finally, coupled system of the equations has the form:

$$\begin{bmatrix} \mathbf{M} & \mathbf{0} \\ \rho \mathbf{S}^{\mathbf{T}} & \mathbf{Q} \end{bmatrix} \begin{Bmatrix} \ddot{\mathbf{u}} \\ \ddot{\mathbf{p}} \end{Bmatrix} + \begin{bmatrix} \mathbf{K} & -\mathbf{S} \\ \mathbf{0} & \mathbf{H} \end{bmatrix} \begin{Bmatrix} \mathbf{u} \\ \mathbf{p} \end{Bmatrix} = \begin{bmatrix} \mathbf{F} \\ \mathbf{q} \end{bmatrix} \tag{6}$$

In equation (6) the matrices $\mathbf{S}$ and $\mathbf{S}^{\mathbf{T}}$ correspond to the forces acting on the fluid – solid boundary, ρ is fluid density and $\mathbf{q}$ is vector that corresponds to the Neumann boundary condition in acoustic equation (pressure amplitude). Those matrices represent the action of the solid inertial forces on the fluid through a common boundary surface, and, on the other side, the action of fluid pressure on the solid domain through the same boundary surface (ANSYS Theory Reference Release 5.6; Morand et al. 1995; Zienkievicz 1983). Those forces are:

$$\mathbf{f}_s = \int_S \bar{\mathbf{N}}^T \mathbf{N} dS \, \mathbf{p} = \mathbf{S}\mathbf{p}$$

$$\mathbf{f}_f = \rho \int_S \bar{\mathbf{N}}^T \mathbf{N} dS \, \ddot{\mathbf{u}} = \rho \mathbf{S}^T \ddot{\mathbf{u}}$$

In the last two equations, matrices $\mathbf{N}$ correspond to linear interpolation of unknown variable and matrices $\bar{\mathbf{N}}$ correspond to weight functions for numerical surface integration. Temporal discretization of the system of equations (6) can be done using Euler's or Newmark's time integration schemes.

However, for vibro-acoustic analysis, the free response of the system is most often considered. In that case, the solution of the system of equations (6) can be assumed in sinusoidal form (Kojic et al. 2010; Bathe 1996):

$$\mathbf{u} = \mathbf{A}_u \sin\left(\omega t + \alpha\right) \tag{7}$$

$$\mathbf{p} = \mathbf{A}_p \sin\left(\omega t + \alpha\right) \tag{8}$$

Substituting equations (7) and (8) in equation (6) produces system of linear equations:

$$\begin{bmatrix} \mathbf{K} - \omega^2 \mathbf{M} & -\mathbf{S} \\ \rho \mathbf{S}^{\mathbf{T}} & \mathbf{H} - \omega^2 \mathbf{Q} \end{bmatrix} \begin{Bmatrix} \mathbf{A}_u \\ \mathbf{A}_p \end{Bmatrix} = \begin{bmatrix} \mathbf{F} \\ \mathbf{q} \end{bmatrix} \tag{8}$$

This system of equations (8) is linear and can be solved by vectors of constants $\mathbf{A}_u$ and $\mathbf{A}_p$. After that, obtained vectors of constants can be replaced in equations (7) and (8) in order to find solutions for displacements or pressure field along with its time derivatives.

Fig. 17 shows computational procedure algorithm used here. The algorithm consists of loading of nodes, elements, prescribed loads and boundary conditions, loop over elements with spatial integration over finite elements and surface integration over solid-fluid interface surface. The algorithm outputs are calculated nodal displacements, nodal pressures and element stresses.

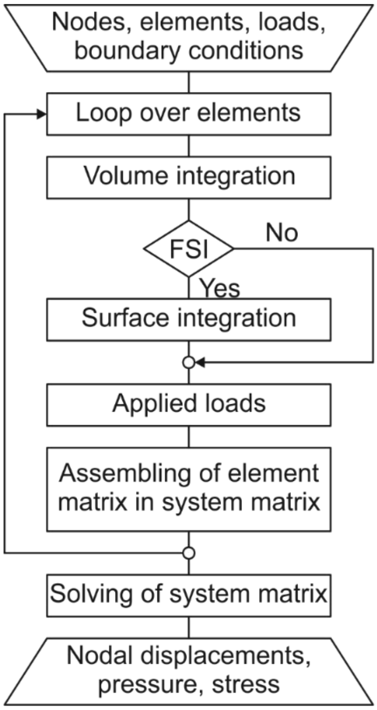

Fig. 17: The Algorithm of the computational procedure

3. Benchmark test

Fluid cavity

The first benchmark test is fluid cavity: modal shapes and natural frequencies. Fluid cavity modal shapes, or acoustic modes, are specific patterns of pressure within a confined fluid volume that occur at discrete natural frequencies. These shapes describe how the fluid oscillates at these frequencies. Three-dimensional fluid cavity is discretized by 8-node brick elements.

The theoretical solution of the natural frequency is given by Beranek et al. 1992.

$$f = \frac{c}{2}\sqrt{\frac{n_1^2}{L^2} + \frac{n_2^2}{W^2} + \frac{n_3^2}{H^2}}, \left(n_1, n_2, n_3 = 0, 1, 2, \ldots\right) \tag{10}$$

where is:

f – natural frequency, c – speed of sound, n_1, n_2, n_3 – natural numbers, L – length of fluid cavity, W – width of fluid cavity, H – height of fluid cavity.

In the simulation, the fluid cavity is assumed to have a rigid boundary condition at each boundary surface. The dimensions of the fluid cavity, mean density of fluid in the cavity and speed of sound propagation in the fluid are given in the **Table 5**.

Dimensions	Length	$0.414m$
	Width	$0.314m$
	Height	$0.360m$
Mean fluid density	ρ_f	$1.21\frac{kg}{m^3}$
Speed of sound	c	$1500\frac{m}{s}$

Table 5: Dimensions and material parameters of the fluid cavity model

The benchmark test is done for the first six natural frequencies. **Table 6** shows calculated values for those natural frequencies: 1. Analytically calculated values, 2. Numerically calculated values in parentheses. The difference between analytical and numerical values them is very small (consequence of a numerical discretization error).

n_1	n_2	n_3	Natural frequency [Hz] (exact value)
0	0	0	0
1	0	0	1811.594203 (1815.13)
0	0	1	2083.333333 (2086.94)
0	1	0	2388.535032 (2392.27)
1	0	1	2760.824394 (2765.85)
1	1	0	2997.828073 (3002.93)

Table 6: Natural frequencies of a fluid cavity: analytical value and numerical value (in parentheses)

Table 6: Natural frequencies of a fluid cavity: analytical value and numerical value (in parentheses) shows the first six natural frequencies and modal shapes of the given fluid cavity. It can be seen that the finite element software gives results very close to the theoretical solution.

Natural frequency	Modal shapes	Scale
1815.13 Hz	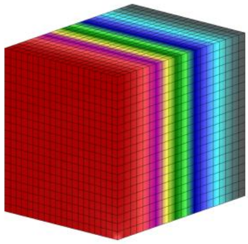	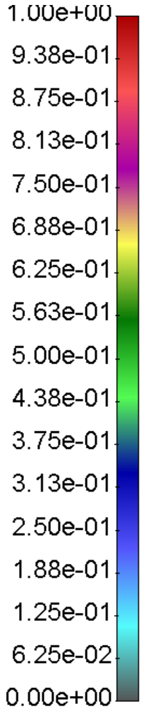
2086.94 Hz	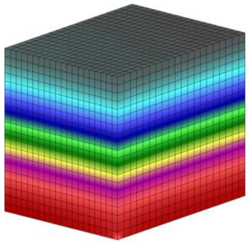	
2392.27 Hz	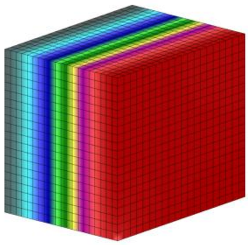	
2765.85 Hz	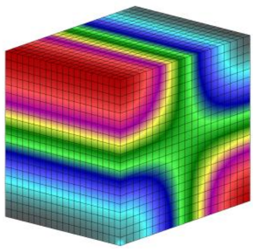	
3002.93 Hz	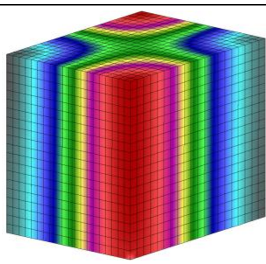	

Table 7: Fluid cavity: natural frequencies and modal shapes. Scale is normalized by value 9.95e-1.

Quadratic solid plate

The second benchmark test is simply supported quadratic solid plate that also includes modal shapes and natural frequencies. Quadratic solid plate modal shapes refer to the vibration patterns (mode shapes) of a three-dimensional, solid plate, where the plate's geometry is described using quadratic finite elements.

There is also analytical solution for natural frequencies in closed form Kojic et al. 2010. The equation for natural frequency is given as:

$$f=\frac{\pi}{2a^2}\sqrt{\frac{D}{\rho h}}\left(m_1^2+m_2^2\right) \tag{11}$$

where is:

a – side length of the quadratic plate,

$D=\frac{Eh^3}{12\left(1-\nu^2\right)}$ – stiffness of the plate,

h – thickness of the plate,

ρ – density of the plate,

m_1, m_2 – natural numbers.

Table 8 shows dimensions of the plate and material properties used as benchmark example.

Dimensions	Plate side	$1.00m$
	Thickness	$0.001m$
Mean fluid density	ρ_f	$1.21\frac{kg}{m^3}$
Young's modulus	E	$2.1\cdot10^{11}Pa$
Poisson's ratio	ν	0.33

Table 8: Dimensions and material properties of vibrating solid plate

Table 9 and **Table 9**: Natural frequencies of a simply supported quadratic plate: analytical value and numerical value (in parentheses)

show natural frequencies and modal shapes obtained by choosing various values for m_1 and m_2. Similar to the fluid cavity example described above, the natural frequencies of simply supported quadratic plate obtained by developed software are very close to the results calculated analytically. This is a proof of the accuracy and reliability of the developed finite element code.

m_2 \ m_1	1	2	3
1	47.986 (47.888)	119.966 (119.885)	239.932 (240.260)
2	119.966 (119.885)	191.946 (191.597)	311.912 (311.667)
3	239.932 (240.260)	311.912 (311.667)	407.885 (409.438)

Table 9: Natural frequencies of a simply supported quadratic plate: analytical value and numerical value (in parentheses)

Natural frequency	Modal shapes	Scale
47.888 Hz	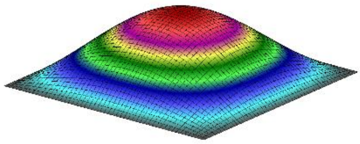	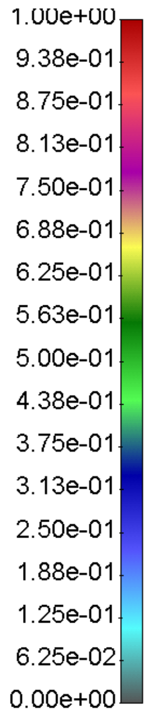
119.885 Hz	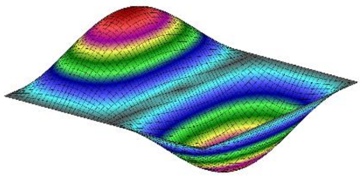	
191.597 Hz	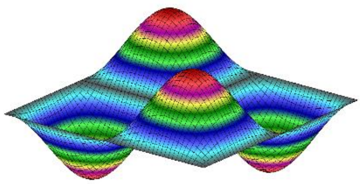	
240.260 Hz	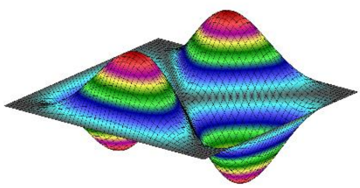	
311.667 Hz	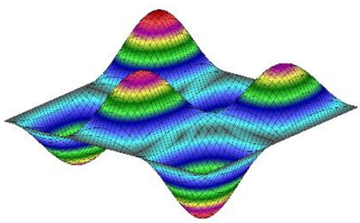	

409.438 Hz	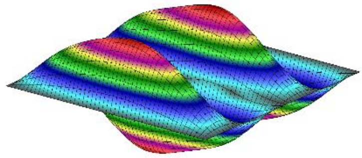	

Table 10: Natural frequencies and modal shapes for simply supported quadratic solid plate. Displacements scale is normalized by value 0.283.

Fluid – solid interaction

The type of problems that include both domains, fluid and solid, does not have solution for natural frequencies in closed form. In order to test coupled system, we made an example based on fluid cavity model. The model consists of a prismatic fluid domain with dimensions given in the **Table 5**. On the upper side, the fluid is in contact with clamped rectangular solid plate. The thickness of the plate is $0.001m$.

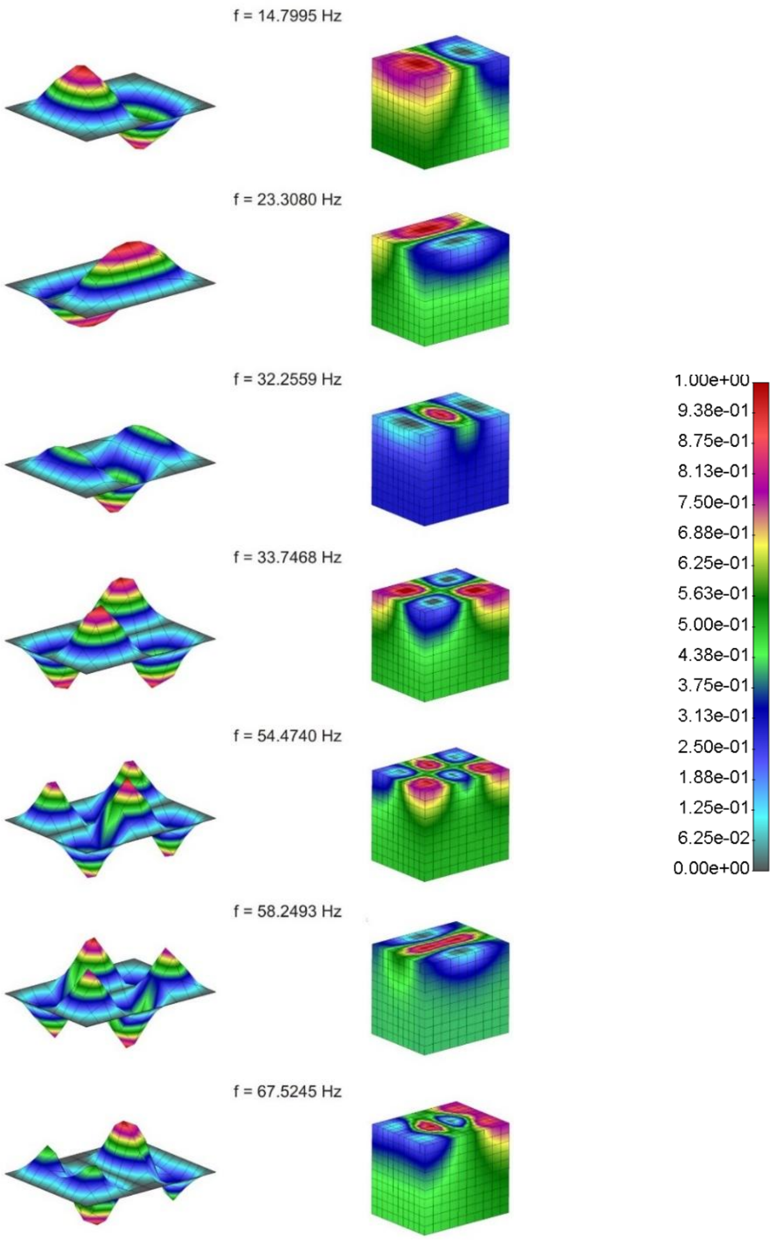

Fig. 18. Natural frequencies and modal shapes for fluid cavity coupled with thin simply supported solid plate (normalized by values: 0.048 for solid and 0.089 for fluid)

Fig. 18 shows natural frequencies and modal shapes for the rectangular clamped solid plate coupled with the fluid below.

Application to the modeling of cochlear mechanics

The main purpose of the development of numerical software presented here was to conduct numerical simulation of a part of the human inner ear – the cochlea. Initial model of the inner ear was taken from the literature (Ni 2012, Ni et al. 2014). Human cochlea is bony structure like a snail shell, with two fluid chambers. Those chambers are separated by basilar membrane (BM). The impulse from the middle ear, generated by acoustic pressure on the ear drum, is transmitted to the cochlea by three ossicles in the middle ear – malleus, incus and stapes. That impulse travels through fluid chambers and causes vibrations of BM.

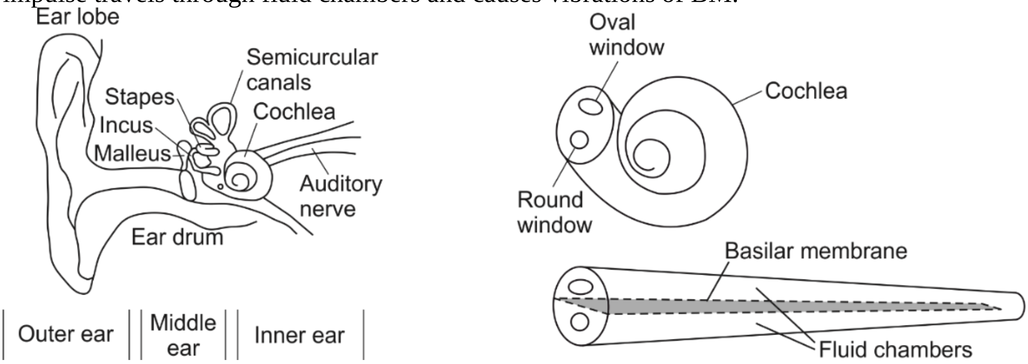

Fig. 19. Human hearing system: Outer, middle and inner ear – cochlea (left); Detail of the cochlear chambers with real coiled geometry and simplified uncoiled geometry (right)

The BM is about 35mm long elastic structure with specific geometry: narrow at the beginning and wide at the end. Consequently, the stiffness is variable along the membrane (high to low, in direction from middle ear to the cochlear apex), allowing for each specific frequency to have an appropriate membrane response. Our simplified model consists of only one fluid chamber and BM. Other parts can be neglected, because they do not affect the response of BM much. Moreover, a simplified uncoiled form of cochlea is used, since it does not affect the results (Ni 2012). Prescribed load is unit force applied at the stapes side of the fluid chamber. Coupling between fluid and solid is achieved through common faces on the fluid – solid boundary surface. The boundary conditions for the BM are three clamped edges and one simply supported edge. These boundary conditions correspond to the real BM, since clamped boundary conditions were applied on the edges where the BM is coupled with bony structure, while simply supported boundary condition was applied on the edge where there is contact between the BM and the spiral ligament (Steele et al. 2002). Material properties used in this model are not investigated here. They are taken from Ni 2012.

The coupling of the fluid and solid domains is achieved by applying boundary condition (5). The simplified geometry of the model is given in **Fig. 20**. In addition to the equations presented in the paper, this model also includes damping. In order to reduce the problem to a simpler form, damping was taken into account through complex stiffness and hysteretic damping factor (Ni 2012; Maia 2009). This is practically modifying of the solid stiffness matrix by an additional complex term. All geometrical and material properties including curves of distribution of Young’s modulus and hysteretic damping coefficient along the BM are used from Ni 2012.

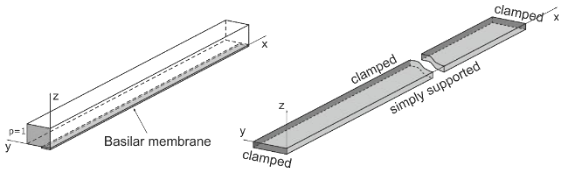

Fig. 20. The geometry of the model of simplified cochlea

Here are given basic geometry quantities (Fig. **20** and **Table 11**), space dependent Young's modulus (as an alternative to the variable geometry) and hysteretic damping coefficient (Fig. **21**).

Fluid chamber cross-section	$1\times1mm$
BM length	$35mm$
BM width	$0.3mm$
BM thickness	$0.05mm$

Table 11: Geometrical properties of the model

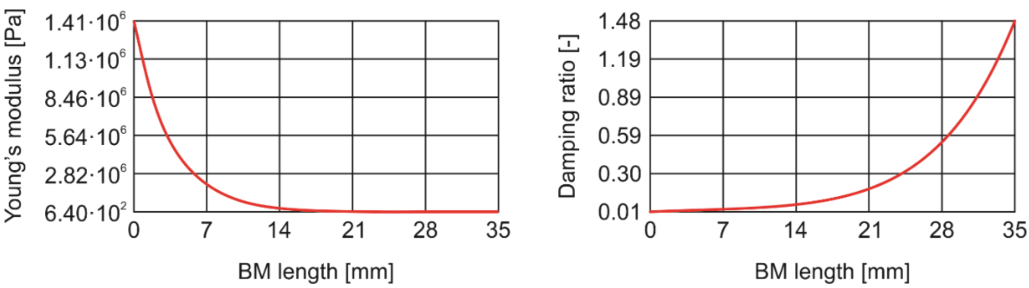

Fig. 21. Young's modulus and damping coefficient distribution along BM

Fig. 22 shows the response of the BM under the excitation frequency of 1 kHz.

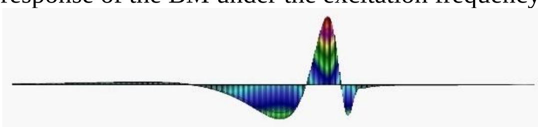

Fig. 22. The response of the BM under the excitation of 1 kHz. The length of membrane is 35 mm. Results are normalized by value 0.0145

As a proof of correctly written numerical software, the distribution of modal velocity amplitude along the BM (**Fig. 23**) is compared with results obtained by WKB method (Steele et al. 2002; Ni 2012). Modal velocity amplitude is the maximum velocity reached during a specific vibration mode of a structure or system, identified by analyzing its response across different frequencies and corresponding to a particular modal shape. Besides that, in the **Fig. 24** is given modal velocity phase for the same model. Modal velocity phase, describes the phase velocity of a wave as it propagates through a complex medium or structure, where the overall wave can be decomposed into distinct modes of vibration. In applications like structural vibration or wave propagation, controlling or understanding modal phase velocity is crucial for optimizing performance or mitigating issues like vibration or signal dispersion.

In the figures 7 and 8 are given modal velocity amplitude and phase for simplified cochlea model. Very small discrepancy between solution calculated by WKB method and numerical solution obtained by FEM software explained here can be explained as a consequence of a numerical discretization error.

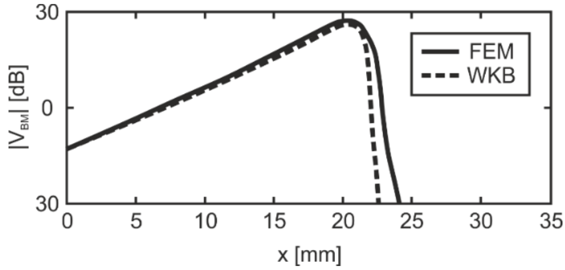

Fig. 23. Comparison of modal velocity amplitude of BM obtained by developed software with WKB method with excitation frequency of 1 kHz.

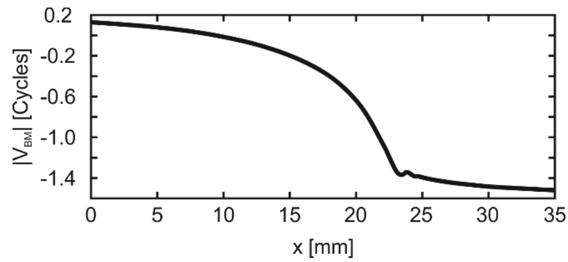

Fig. 24. Modal velocity phase of BM calculated by developed software with excitation frequency of 1 kHz.

In addition to this simple example, a more complex model that contains elements of the middle and inner ear was made. This model has more realistic geometry, material properties and boundary conditions. All those data are taken from Homma et al. 2009, Kim et al. 2011 and Tachos et al. 2016. Cochlea and BM have variable geometry along its length in order to obtain response which corresponds to the real BM behavior. Boundary condition is prescribed displacements in both three directions, X, Y, Z with value of 0.01 µm. For such a boundary condition, which corresponds to the transmission of sound through the bones, the frequency response of the whole system is observed. In **Fig. 25** are given: 1. geometry of the model with different materials, 2. contour plot of nodal displacements obtained by developed software and modal velocity magnitude of BM. The distribution of modal velocity magnitude along BM is also validation of the software solution described in this paper. The diagram in **Fig. 25** shows comparison of results obtained by our software (PAK, Kojic et al. 2017) with COMSOL software used in Homma et al. 2009 and Kim et al. 2011. There is a small difference due to the spatial discretization of models which are not completely identical in terms of the finite element mesh. The result shown here is one more proof of accuracy of the developed software, since results show very good agreement with results obtained by commercial software COMSOL.

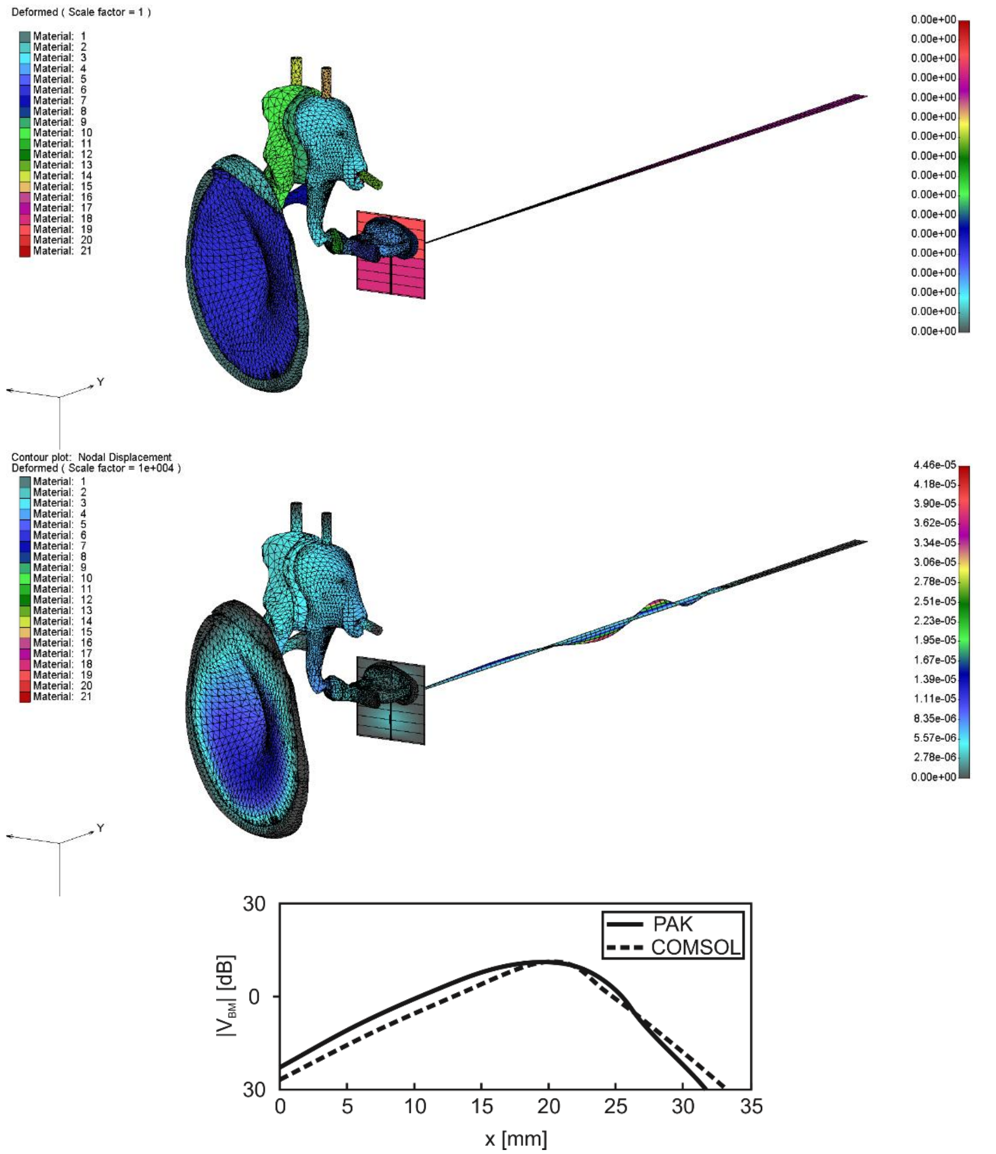

Fig. 25. Finite element model of the middle and inner ear. Geometrical and material data, boundary conditions and prescribed loads are used from Homma et al. 2009 and Kim et al. 2011

The model presented here is simplification of real human hearing system. This model can be upgraded with more appropriate material models for ligaments and bones. But, the most sensitive and the most significant part in this model is model of BM. The real geometry of BM is not too complex, but real material properties of BM material are very anisotropic. Both of these things need to be adjusted to get the appropriate mechanical response of BM. At the current stage of general research in this field is not possible to “measure” and apply real material properties. It is only possible to fit material (or geometrical) properties in order to obtain mechanical response that corresponds to the real behavior of the cochlea and BM.

4. Conclusion

This paper presents part of research done during successfully finished SIFEM project. One of the main project objectives was developing of software solution for modeling of inner ear. The scientists engaged in research related to the modeling of the middle and inner ear (Böhnke et al. 1999; Chang et al. 2018; Kamieniecki et al. 2017) most commonly use software such as ANSYS (ANSYS Multiphysics module) or COMSOL (COMSOL Multiphysics, Structural Mechanics & Acoustics Modules). The numerical software presented here is result of the research on the mentioned project. However, it is general purpose software and can be applied for modeling in other fields of science considering that acoustic – structure problems occur in various fields of science and technology. The software is developed based on three-dimensional fluid and solid finite elements, but can be easily extended by other types of elements, especially structural elements like shells, beams, rods, etc. Furthermore, the domain of solid and fluid can be completely arbitrary, given that a finite element method with 3D elements was used. The code is uploaded into a public repository of software solutions resulting from the scientific research done during projects from FP7 calls, making it publicly available to the scientists interested in using and further development of such a software solution.

Acknowledgement. This work was supported in part by grants from Serbian Ministry of Education and Science III41007, ON174028 and FP7 ICT SIFEM 600933. The result reflects only the author's view and the European Commission is not responsible for any use that may be made of the information it contains.

Appendix

In **Table 12** is given nomenclature used in the paper.

Symbol	Description
p	Acoustic pressure
x_i	Spatial (Cartesian) coordinates
t	Time
c	Speed of sound (in acoustic wave equation)
$\mathbf{Q}$	Acoustic inertia
$\mathbf{H}$	Acoustic stiffness
$\mathbf{N}$	Pressure shape functions
$\mathbf{N}'$	Pressure shape functions derivatives
$\mathbf{M}$	Mass matrix
$\mathbf{C}$	Damping matrix
$\mathbf{K}$	Stiffness matrix
$\mathbf{D}$	Elasticity matrix
$\mathbf{u}$	Solid displacements
$\dot{\mathbf{u}}$	Solid velocities
$\ddot{\mathbf{u}}$	Solid accelerations
$\mathbf{F}^{\mathbf{ext}}$	External forces
$\mathbf{B}$	Strain-displacement matrix

ρ	Solid density
c	Damping coefficient (in Newtonian equation of motion)
$\mathbf{n}$	Normal vector
ω	Angular frequency
α	Phase shift
f	Natural frequency
ρ_f	Fluid density

Table 12: Nomenclature

References

Amestoy P, Duff I, L'Excellent YI and Koster J. A Fully Asynchronous Multifrontal Solver Using Distributed Dynamic Scheduling. *SIAM J. Matrix Anal. Appl*. 1999. 23(1), 15–41.

ANSYS Theory Reference, Edited by Peter Kohnke, Release 5.6, ANSYS Inc.

ANSYS Multiphysics module https://www.ansys.com/products/platform/multiphysics-simulation

Bathe KJ. *Finite Element Procedures*. Prentice-Hall, Englewood Cliffs, N. J., 1996.

Beranek LL and Vér IL. *Noise and Vibration Control Engineering*. John Wiley & Sons, Inc. New York, 1992.

Böhnke F, Arnold W. 3D-Finite Element Model of the Human Cochlea Including Fluid-Structure Couplings, *ORL J Otorhinolaryngol Relat Spec*. 1999;61:305–310

Chang Y, Kim N, Stenfelt S. Simulation of the power transmission of bone-conducted sound in a finite-element model of the human head. *Biomechanics and Modeling in Mechanobiology*, 2018. Volume 17, Issue 6, pp 1741–1755.

COMSOL Multiphysics, Structural Mechanics & Acoustics Modules https://www.comsol.com/

Homma K, Du Y, Shimizu Y, Puria S. Ossicular resonance modes of the human middle ear for bone and air conduction. *J Acoust Soc Am*. 2009 Feb;125(2):968-79. doi: 10.1121/1.3056564. PMID: 19206873; PMCID: PMC2852437.

Isailovic V., Kojic M., Milosevic M., Filipovic N., Kojic N., Ziemys A., Ferrari M., A computational study of trajectories of micro- and nano-particles with different shapes in flow through small channels, Journal of the Serbian Society for Computational Mechanics, Vol. 8 No. 2, pp.14-28 UDC: 532.517.2, 2014.

Kamieniecki K, Piechna J, Borkowski P, Basilar Membrane Vibration in Time Domain Predicted by Fluid–Structure Interaction Model in Pre- and Post-stapedotomy State. *Procedia IUTAM* Elsevier 2017. Vol. 24.

Kim, N., Homma, K. & Puria, S. Inertial Bone Conduction: Symmetric and Anti-Symmetric Components. *JARO* 12, 261–279 (2011). https://doi.org/10.1007/s10162-011-0258-3

Kojic M, Slavkovic R, Zivkovic M, Grujovic N. *Finite Element Method – Linear analysis*. Faculty of mechanical engineering, University of Kragujevac, 2010.

Kojic M, Filipovic N, Stojanovic B, Kojic N. *Computer Modeling in Bioengineering – Theoretical Background, Examples and Software*. John Wiley and Sons, 978-0-470-06035-3, England, 2008.

Kojic M, Slavkovic R, Zivkovic M, Grujovic N, Filipovic N. PAK, *Finite element software*, BioIRC Kragujevac, University of Kragujevac, 34000 Kragujevac, Serbia.

Kojic M., Milosevic M., Kojic N., Isailovic V., Petrovic D., Filipovic N., Ferrari M., Ziemys A., Transport phenomena: Computational models for convective and diffusive transport in capillaries and tissue, in: Suvranu De, Wonmuk Hwang, Ellen Kuhl, Eds., Multiscale Modeling in Biomechanics and Mechanobiology, Springer, Chapter 7, 131-156, 2015.

Maia N. Reflections on the hysteretic damping model. *Shock and Vibration* 2009. Vol 16. pp. 529–542.

Morand H, Ohayon R. *Fluid Structure Interaction. Applied Numerical Methods*. Chichester etc., John Wiley & Sons; Paris etc., Masson 1995.

Ni G. Fluid coupling and waves in the cochlea. PhD thesis. University of Southampton, Faculty of engineering and the environment, Institute of sound and vibration research, 2012.

Ni G, Elliott SJ, Ayat M and Teal PD. Modelling Cochlear Mechanics, *Hindawi Publishing Corporation, BioMed Research International*, 2014.

Rienstra SW and Hirschberg A, *An Introduction to Acoustics*, Eindhoven University of Technology, Eindhoven, 2009.

Steele C, Baker G, Tolomeo J, Zetes-Tolomeo D. Cochlear Mechanics. In: Schneck DJ, Bronzino JD. *Biomechanics – Principles and Applications* 2002. DOI:10.1201/9781420040029.ch18,

Steele C and Taber L. Comparison of WKB calculations and finite difference calculations for a two-dimensional cochlear model. *The Journal of the acoustical Society of America* 1979. 65(4), 1001-1006

Tachos, N.S., Sakellarios, A.I., Rigas, G., Isailovic, V., Ni, G., Böhnke, F., Filipovic, N., Bibas, T., and Fotiadis, D.I., Middle and inner ear modelling: From microCT images to 3D reconstruction and coupling of models, *IEEE 38th Annual International Conference of the IEEE Engineering in Medicine and Biology Society (EMBC)*, Page(s): 5961-5964, August 16-20, 2016. ISBN: 978-1-4577-0220-4, doi: 10.1109/EMBC.2016.7592086

Zienkievicz O. *The finite element method (third edition)*, McGraw-Hill Book Co., New York, 1983.